RESEARCH ARTICLE

Robust Optimization for Microgrid Management With Compensator, EV, Storage, Demand Response, and Renewable Integration

HAMID HEMATIAN[1], MOHAMAD TOLOU ASKARI [1], MEYSAM AMIR AHMADI[1], MAHMOOD SAMEEMOQADAM [2], AND MAJID BABAEI NIK[1]

[1]Department of Electrical Engineering, Islamic Azad University, Semnan Branch, Semnan 3513119111, Iran
[2]Department of Electrical Engineering, Islamic Azad University, Shahrood Branch, Shahrood 3619943189, Iran

Corresponding author: Mohamad Tolou Askari (m.asgari@gmail.com)

ABSTRACT Navigating the complex terrain of microgrid energy management is challenging due to the uncertainties linked with abundant renewable resources, fluctuating demand, and a wide range of devices including batteries, distributed energy sources, electric vehicles, and compensatory devices. This paper presents an advanced two-stage robust day-ahead optimization model designed specifically for MG operations. The model primarily addresses challenges arising from the integration of power electronics-based generation units, the unpredictable nature of demand in microgrids, and the integration of small-scale renewable energy sources. The proposed model includes detailed formulations for MG energy management, covering optimal battery usage, efficient EV energy management, compensator usage, and strategic dispatching of DG resources. The multi-objective function aims to minimize various costs related to energy losses, power purchases, load curtailment, DG operation, and battery/EV expenses over a 24-hour period. To efficiently solve this optimization problem, the C&CG algorithm is utilized. Numerical simulations on a test system validate the effectiveness of the proposed model and solution algorithm, showing a significant reduction in the operating costs of the microgrid. This approach offers a robust framework to enhance the resilience and efficiency of microgrid energy management. The results conclusively demonstrate that the proposed approach surpasses comparable methods by at least 5%, highlighting its effectiveness in improving key indicators within the microgrid system.

INDEX TERMS Microgrid, two-stage robust optimization, demand response, storage, electric vehicle, uncertainty.

NOMENCLATURE

A. SET AND INDEX

N	Set of grid nodes, indexed by n.
B	Set of grid lines, indexed by nm.
T	Set of hour of a day, indexed by t.
M	Set of step rate for OLTC and SVR, indexed by m.
Ω^{OLTC}	Placement of the OLTC bus in the power system.
Ω^{SVR}	Placement of the SVR bus in the power system.

B. PARAMETERS

R_{nm}, X_{nm}	Resistance and reactance of line, respectively .
$\overline{F}^p_{nm,t}, \overline{F}^q_{nm,t}$	Maximum active and reactive power flow of the line, respectively.
c^{sub}_t	Cost of purchasing power from the substation.
c^{shed}_t	Cost of load shedding.
c^{loss}_t	Cost of power losses.
c^{DG}_t	Cost of DG operation.
c^{ess}_t	Cost of ESS operation.
c^{ev}_t	Cost of EV operation.

$D_{n,t}^{p,INI}, D_{n,t}^{q,INI}$	Initial active and reactive load of the network, respectively.
$\tilde{P}_{n,t,s}^{RE}$	Real power output of renewable energy sources in different scenarios.
ρ	Power factor of distributed generation.
γ	Load change percentage in demand side management program.
C_n^{ess}	Battery capacity.
$\underline{soc}_n^{ess}, \bar{soc}_n^{ess}$	Minimum and maximum of SOC of the battery, respectively.
$\bar{Q}_n^{sc}, \bar{Q}_n^{ShR}$	Maximum reactive power of SC and ShR, respectively.
$\nabla_{n,t,m}^{oltc}, \nabla_{n,t,m}^{SVR}$	Taps rate of OLTC and SVR, respectively.
A_m, B_m	Set of steps rate considered for OLTC and SVR, respectively.
$\bar{P}_n^{EV,cha}, \bar{P}_n^{EV,dis}$	Maximum charging and discharging power of the electric vehicle battery, respectively.
$\eta_{EV}^{ch}, \eta_{EV}^{dis}$	Efficiency of electric vehicles battery charging and discharging.
$\bar{E}_n^{EV}$	Maximum battery capacity in electric vehicles.
E^{soc}	Minimum SOC status of the EV in percent.

C. VARIABLES

P_t^{sub}, Q_t^{sub}	Real and reactive power of the substation.
$D_{n,t}^{p,DSM}, D_{n,t}^{q,DSM}$	Real and reactive demand changed in the DSM program, respectively.
$P_{n,t}^{RE}$	Operated power of renewable energy resources.
$P_{n,t}^{ess,cha}, P_{n,t}^{ess,dis}$	Charge and discharge power of the battery, respectively.
$P_{n,t}^{DG}$	Real power of distributed generation.
$E_{n,t}^{ess}$	Energy level of the battery.
$\eta^{ess,cha}, \eta^{ess,dis}$	Charge and discharge efficiency of the battery, respectively.
$Q_{n,t}^{sc}, Q_{n,t}^{ShR}$	Reactive power of SC and ShR, respectively.
$P_{n,t}^{EV,cha}, P_{n,t}^{EV,dis}$	Charging and discharging power of electric vehicles, respectively.
$E_{n,t}^{EV}$	Energy status in the battery of electric vehicles.

D. BINARY VARIABLES

$z_{n,t}$	Battery charge status.
y_{nm}	Auxiliary binary variable for reconfiguration.
$\varphi_{n,t}$	The active status of the SC is indicated by a value of 1, otherwise, it is zero, which denotes the active status of ShR.
$\theta_{m,t}^{SVR}, \theta_{m,t}^{oltc}$	Extra binary variables for SVR and OLTC steps.

$\gamma_{n,t}$	Status of charging and discharging of electric vehicles, if it is equal to 1, the electric vehicle is charging, otherwise, it indicates the status of discharging.

E. ABBREVIATIONS

ADMM	Alternating Direction Method of Multipliers.
BD	Benders Decomposition.
ML	Machine learning.
MG	Microgrid.
EV	Electric Vehicle.
DG	Distributed generation.
C&CG	Column-and-constraint generation.
ADPM	Adaptive Dynamic Power Management.
EISCT	Enhanced Instantaneous Symmetrical Component Theory.
OHPF	Optimal harmonic power flow.
PQ	Power quality.
MINLP	Mixed integer non-linear programming.
MMG	Multi-microgrids.
BESS	Battery Energy Storage Systems.
PCBGA	Beasley parallel genetic algorithm.
HSA	Harmony search algorithm.
IEMs	Integrated energy microgrids.
P2P	Peer-to-Peer.
MMG	Multi-microgrid.
BDCs	Bidirectional converters.
DN	Distribution network.
DR	Demand response.
MILP	Mixed-Integer Linear Programming.
OLTC	On-Load Tap Changer.
SVR	Step Voltage Regulator.
PV	Photovoltaic.
EVPL	Electric vehicle parking lots.
ESS	Energy storage system.
SC	Shunt capacitor.
ShR	Shunt reactor.
WD	Wind resource.

I. INTRODUCTION

The global energy landscape is undergoing a significant transformation, with microgrids emerging as key players in the quest for sustainable, resilient, and decentralized energy solutions. Microgrids, which are localized and often interconnected energy systems, offer a promising approach to meeting the changing needs of communities, industries, and critical infrastructure. However, integrating and managing diverse energy resources within microgrids pose significant challenges, amplified by the inherent uncertainties of renewable sources, fluctuating demand patterns, and the inclusion of various devices such as batteries, distributed energy sources, electric vehicles, and compensatory devices. In this complex context, this paper aims to address the critical issues hindering optimal microgrid energy management. A central focus is placed on developing an advanced two-stage

robust day-ahead optimization model specifically tailored for MG operations. This model is designed to navigate and overcome challenges associated with integrating power electronics-based generation units, the unpredictable demand nature within microgrids, and the incorporation of small-scale renewable energy resources.

A. BACKGROUND REVIEW

In [1], an ADPM and EISCT are introduced to tackle challenges in PV-wind-battery microgrids, addressing issues like poor power quality and grid instability. In [2], an OHPF framework for daily scheduling of a grid-connected microgrid is presented, which tackles PQ issues caused by power electronics and unbalanced loading. In [3], a bi-objective optimization approach based on the MINLP framework is proposed to enhance microgrid resilience using the power-to-hydrogen concept, enabling autonomous operation. In [4], a fully decentralized adjustable robust operation framework is proposed for active distribution networks with MMG, addressing the autonomy and heterogeneity of individual agents. In [5], a Stackelberg game approach is proposed for robust microgrid energy sharing, incorporating prosumers and plug-in electric vehicle charging stations while considering uncertainties in renewable energy, storage systems, and load consumption. In [6], a MINLP model is proposed for optimal placement, technology selection, and operation of BESS in microgrids, considering variable distributed generation and energy demand using a methodology with PCBGA. In [7], a low-carbon operation method is proposed for microgrids, addressing the challenge of high carbon emissions by considering energy-carbon coupling units such as distributed generators and industrial loads. In [8], the authors propose an optimal capacitor allocation approach in islanded microgrids using HSA. In [9], the authors propose a low-carbon economy operation strategy for multiple IEMs based on a double-layer Stackelberg game model. In [10], the authors develop a data-driven scheduling-correction framework for renewable-dominated isolated microgrids integrated with hybrid seasonal battery storage. In [11], the authors develop a multi-microgrid P2P low-carbon economic operation model based on Nash bargaining theory, considering the coordination of three energy forms (electricity, heat, and gas), uncertainties on both sides of the source and load, and low-carbon operation goals. In [12], a two-stage distributionally robust model is proposed for the optimal design and operation of islanded MMG systems using a C&CG-based method. In reference [13], the proposed use of digital platforms for automating the reliability assessment of microsystems in modern energy technologies involves employing machine learning methods with two algorithms designed to analyze regime indicators and assess reliability. In [14], a data-based convex model is proposed for the performance of AC/DC hybrid microgrids with bidirectional converters using the least squares approximation method with data-based weight functions to linearize BDC efficiency behavior. In [15],

a dedicated microgrid planning and operation approach is proposed, especially to support a DN with pumped hydraulic storage. In [16], a grid-connected microgrid power optimization model based on the integration of microgrid and electric vehicles is proposed using an adaptive crossover multi-particle swarm optimization algorithm. In [17], the unexplored potential of multi-energy microgrids as virtual power plants in auxiliary service markets is addressed using Stackelberg game theory and integrated DR. In [18], a price-based strategy for coordinating electric springs in microgrids is proposed, focusing on the economic benefits of smart loads. In [19], a stochastic multi-objective optimization approach is presented for optimal performance and coordination of energy hubs, renewable energy sources, and plug-in electric vehicles in smart microgrids. In [20], an extensive review of literature is provided on the energy management of microgrid control systems, discussing challenges in overall control and stable operation. Studies [21] and [22] have introduced column and constraint generation algorithms for robust optimization models. References [23] and [24] have presented a robust optimization model for microgrid island operation. In [25], a stochastic model for robust optimization in the presence of demand response management problems is presented. In [26], an improved energy management strategy for customer buildings is proposed to minimize microgrid operating costs and battery degradation factors. In [27], a two-layer approach is presented to manage and control an AC microgrid with photovoltaic systems, wind turbine systems, and battery storage systems connected to the power grid. In [28], the development of a model for optimizing the use of local clean energy sources in a microgrid for grid connection has been investigated. The study [29] provides an overview for researchers on predictive control methods for economic modeling of microgrids to achieve objectives such as cost minimization and profit maximization. In [30], the two-mode energy management problem in microgrid coordination has been investigated. The paper introduces a two-stage robust approach for optimizing operation and coordination in microgrids. The methodology utilizes MILP for robustness, C&CG for optimization, and integrates various components such as EVs, ESS, compensators, demand response, reactive loads, and renewable sources. The approach presented in the paper, which combines MILP and C&CG, offers a comprehensive and robust solution for microgrid operation. It addresses multiple objectives and incorporates a variety of elements. Table (1) showcases the versatility of the proposed model, surpassing other studies in addressing diverse challenges and integrating a broad spectrum of components to enhance microgrid performance. Many studies lack a robust approach, as evidenced by the absence of "Robust" in the "Approach" column, which may leave them susceptible to uncertainties and variations in microgrid conditions. Some studies also lack the comprehensive integration of essential microgrid components. For example, [10] and [13] do not consider compensators, [6] excludes EVs, and [14] does not incorporate

TABLE 1. Comparison of the approach and model of this paper with similar.

Ref.	Model	Approach	Algorithm	Multi-Objective	EV	ESS	Compensator	Demand Response	Reactive Load	Renewable
This paper	MILP	Robust	C&CG	✓	✓	✓	✓	✓	✓	✓
[1]	NLP	Deterministic	-	-	-	✓	-	-	✓	✓
[2]	MILP	Deterministic	Heuristic	✓	✓	✓	-	✓	✓	✓
[3]	MINLP	Deterministic	BD	✓	-	-	-	-	✓	✓
[4]	MIQP	Robust	ADMM	✓	-	✓	-	-	✓	✓
[5]	MINLP	Robust	Stackelberg	-	✓	✓	-	✓	-	✓
[6]	MINLP	Deterministic	Metaheuristic	✓	-	✓	-	-	-	-
[7]	MILP	Deterministic	-	-	-	✓	-	-	✓	✓
[8]	NLP	Deterministic	Evolutionary	-	-	-	✓	✓	✓	-
[9]	NLP	Robust	Stackelberg	-	-	✓	-	-	-	✓
[10]	NLP	Deterministic	data-driven	-	-	✓	-	-	-	✓
[11]	MINLP	Robust	ADMM	-	-	-	-	-	-	✓
[12]	MILP	Robust	C&CG	-	-	-	-	-	-	✓
[13]	NLP	Deterministic	ML	-	-	✓	-	-	-	✓
[14]	LP	Deterministic	data-driven	-	-	-	-	-	✓	✓
[15]	NLP	Deterministic	dedicated	-	-	✓	-	-	-	✓
[16]	NLP	Deterministic	Evolutionary	✓	✓	✓	-	-	-	✓
[17]	NLP	Robust	Stackelberg	✓	-	✓	-	✓	-	✓
[18]	MINLP	Deterministic	Heuristic	✓	-	✓	-	✓	-	✓
[19]	NLP	Stochastic	Evolutionary	✓	✓	✓	-	✓	-	✓

demand response. Several studies struggle to address multiple objectives simultaneously. Specifically, [3], [5], [11], [12], and [17] do not explicitly include all the listed objectives (Multi-Objective) in their approach.

B. MOTIVATION

The paper is motivated by the need to address the complex challenges associated with microgrid energy management, particularly amidst increasing uncertainties related to renewable resources, dynamic demand patterns, and the diverse array of devices found in microgrids, such as batteries, distributed energy sources, electric vehicles, and compensators. The authors emphasize the necessity for a sophisticated optimization model tailored specifically for microgrid operations. The primary challenges they aim to address include integrating power electronics-based generation units, managing the uncertain demand nature within microgrids, and effectively incorporating small-scale renewable energy resources. These challenges require a comprehensive approach to energy management within microgrids. The proposed two-stage robust day-ahead optimization model focuses on several key aspects of microgrid energy management. It aims to optimize battery usage, manage EV energy efficiently, utilize compensators effectively, and strategically dispatch distributed generation (DG) resources. The authors stress the importance of addressing a multi-objective function aimed at minimizing various costs related to energy losses, power purchases, load curtailment, DG operation, and expenses associated with batteries and electric vehicles over a 24-hour period. To solve this optimization problem efficiently, the paper introduces the use of a C&CG algorithm. The authors validate the effectiveness of their proposed model and solution algorithm through numerical simulations conducted on a test system. The results show a significant reduction in the microgrid's operating cost, supporting the claim that the proposed approach enhances the efficiency of microgrid energy management while providing a robust framework to strengthen the resilience of the microgrid system. In summary, the paper aims to offer a comprehensive solution to the intricate challenges of microgrid energy management, providing a specialized two-stage optimization model and algorithm to address uncertainties, optimize resource usage, and minimize costs. Ultimately, this enhances the efficiency and resilience of microgrid operations.

C. RESEARCH GAP

While there has been significant research in the field of microgrid energy management, the existing body of literature presents several limitations and gaps that necessitate further investigation and innovation.

1. Limited Integration of Multiple Energy Resources:

- Many existing studies focus on individual aspects of microgrid management, such as renewable energy integration or demand response, without considering the holistic integration of multiple energy resources, electric vehicles, and storage systems.

2. Simplistic Optimization Models:

- Several studies employ simplistic optimization models that do not capture the complexities, uncertainties, and dynamic nature of microgrid operations effectively. These

TABLE 2. Grid-Connected mode result.

	Proposed	Method 1 in [24]	Method 2 in [25]
Objective ($)	86978	93936	91326
Energy purchase (MWh)	0.45	0.474	0.468
Loss (MWh)	0.387	0.410	0.405
Load shedding (MWh)	0.16	0.388	0.319
Voltage deviation (p.u)	0.065	0.068	0.068
PV curtailment (MWh)	2.25	2.31	2.27
WD curtailment (MWh)	0	0.15	0
Peak of charge of ESS (MWh)	0.56	0.59	0.58
Total power of the SC (MVArh)	10.66	10.87	10.80
Total power of the ShR (MVArh)	11.4	11.2	11.24
CPU time (sec)	131	97	61

models often overlook critical factors such as grid stability, voltage regulation, and real-time adaptation.

3. Lack of Robustness and Adaptability:

- The majority of existing models lack robustness and adaptability to handle uncertainties in renewable energy generation, demand variations, and equipment failures. This results in suboptimal performance and reliability under diverse operating conditions.

4. Limited Scalability and Flexibility:

- Many studies focus on specific microgrid configurations or scenarios, limiting their applicability and scalability to different microgrid sizes, configurations, and operational requirements.

Given these limitations, there is a clear research gap and need for innovative approaches that address the complexities and challenges of modern microgrid operations comprehensively.

Our proposed two-stage optimization model aims to fill these gaps by:

- Providing a holistic and integrated approach to microgrid energy management.
- Incorporating advanced optimization techniques to handle uncertainties and dynamic operational conditions effectively.
- Ensuring robustness, adaptability, and scalability to meet the diverse requirements of various microgrid applications.

By addressing these limitations and providing a tailored solution for microgrid operations, this research contributes significantly to advancing the state-of-the-art in microgrid energy management and addressing the identified research gaps. However, to demonstrate the research gap and differences as well as the advantages, the proposed paper is designed in Table (1).

D. RESEARCH CONTRIBUTION

The paper makes a significant contribution to the field of microgrid operations by addressing a specific research gap and proposing a sophisticated and robust optimization model. Here are the key contributions and their explanations:

- The paper introduces a detailed formulation for microgrid energy management that encompasses various aspects, including optimal battery usage, efficient electric vehicle energy management, compensator usage, and strategic dispatching of distributed generation resources.

- The proposed model incorporates a multi-objective function aimed at minimizing various costs related to energy losses, power purchases, load curtailment, distributed generation operation, and expenses associated with batteries and electric vehicles. This reflects a comprehensive approach to microgrid energy management.

- The paper makes a methodological contribution by utilizing a column-and-constraint generation algorithm for efficient optimization. This algorithm is specifically highlighted as addressing the identified research gap, indicating an innovative approach to tackling the complexities of microgrid energy management.

- The energy management structure of microgrids is accurately modeled through a well-structured MILP, demonstrating a high level of detail and precision in representing the intricacies of microgrid operations.

E. PAPER ORGANIZATION

In the following sections of this paper, we will introduce the proposed modeling, followed by an explanation of the problem-solving methodology. We will then analyze the simulation results and conclude by offering suggestions for future research directions.

II. PROPOSED MODEL

The presented optimization problem focuses on comprehensive microgrid energy management, taking into account factors such as optimal battery operation, efficient EV energy management, compensator usage, and strategic dispatching of DG resources. The multi-objective function aims to minimize costs associated with energy losses, power purchases, load curtailment, DG operation, and expenses related to batteries and electric vehicles over a 24-hour period. The model incorporates various equations and inequalities that represent the balance of real and reactive power, restrictions on using power from the upstream network, demand-side management constraints, considerations for flexible loads, adjustments in active and reactive power, voltage limits, energy storage system modeling, operational limits for renewable resources, capacitor and shunt reactor limits, and optimal settings for OLTC and SVR.

In the optimization problem presented, various aspects of microgrid energy management are addressed, such as optimal battery charging and discharging, efficient EV energy management, effective compensator usage, strategic management of SVR and OLTC, and strategic dispatching of DG resources. Additionally, the model takes into account load variations. The multi-objective function, defined by Equation (1), seeks to minimize several factors: the cost of

energy losses over 24 hours, power purchase costs from the upstream grid, load curtailment costs, DG operation costs, and battery and EV operational expenses.

$$\min \sum_{nm \in B} \sum_{t \in T} c_t^{loss} R_{nm} \left({F_{nm,t}^p}^2 + {F_{nm,t}^q}^2 \right) T$$
$$+ \sum_{t \in T} c_t^{sub} \left(P_t^{sub} + Q_t^{sub} \right)$$
$$+ \sum_{n \in N} \sum_{t \in T} c_t^{shed} \left(D_{n,t}^{p,shed} + D_{n,t}^{q,shed} \right)$$
$$+ \sum_{n \in N} \sum_{t \in T} c_t^{DG} \left(P_{n,t}^{DG} \right) + \sum_{n \in N} \sum_{t \in T} c_t^{ess} \left(P_{n,t}^{ess,ch} + P_{n,t}^{ess,dis} \right)$$
$$+ \sum_{n \in N} \sum_{t \in T} c_t^{ev} \left(P_{n,t}^{EV,ch} + P_{n,t}^{EV,dis} \right) \tag{1}$$

Equations (2) and (3) illustrate the equilibrium of real and reactive power within the microgrid.

$$P_t^{sub} + P_{n,t}^{ess,dis} - P_{n,t}^{ess,ch} + \sum_{nm \in B(n)} F_{nm,t}^p - \sum_{nm \in B(n)} F_{mn,t}^p$$
$$+ P_{n,t}^{DG} + P_{n,t}^{RE} + D_{n,t}^{p,shed} - D_{n,t}^{p,DSM}$$
$$- P_{n,t}^{EV,ch} + P_{n,t}^{EV,dis} = 0 \forall n \in N, t \in T, nm \in B \tag{2}$$
$$Q_t^{sub} + \sum_{nm \in B(n)} F_{nm,t}^q - \sum_{nm \in B(n)} F_{mn,t}^q + \rho \times P_{n,t}^{DG}$$
$$+ D_{n,t}^{q,shed} - D_{n,t}^{q,DSM} + Q_{n,t}^{sc} - Q_{n,t}^{ShR} = 0 \ \forall n \in N,$$
$$t \in T, b \in B \tag{3}$$

Inequalities (4) and (5) indicate the restrictions on utilizing active and reactive power from the upstream network, respectively.

$$\underline{P}^{sub} \le P_t^{sub} \le \overline{P}^{sub} \forall t \in T \tag{4}$$
$$\underline{Q}^{sub} \le Q_t^{sub} \le \overline{Q}^{sub} \forall t \in T \tag{5}$$

Equations (6) and (7) specify the constraints on the total active and reactive loads within the demand-side management program. These relationships imply that, in the demand-side management program, the total microgrid load can be less than the initial network loads. Essentially, this indicates the consideration of flexible loads in this study.

$$\sum_{n \in N} D_{n,t}^{p,DSM} \le \sum_{n \in N} D_{n,t}^{p,INI} \forall t \in T \tag{6}$$
$$\sum_{n \in N} D_{n,t}^{q,DSM} \le \sum_{n \in N} D_{n,t}^{q,INI} \forall t \in T \tag{7}$$

Inequalities (8) and (9) express the magnitude of active and reactive adjustments within the demand-side management plan, respectively.

$$D_{n,t}^{p,INI} - D_{n,t}^{p,INI} \times \gamma \le D_{n,t}^{p,DSM} \le D_{n,t}^{p,INI} + D_{n,t}^{p,INI}$$
$$\times \gamma \forall n \in N, t \in T \tag{8}$$
$$D_{n,t}^{q,INI} - D_{n,t}^{q,INI} \times \gamma \le D_{n,t}^{q,DSM} \le D_{n,t}^{q,INI} + D_{n,t}^{q,INI}$$
$$\times \gamma \forall n \in N, t \in T \tag{9}$$

Constraints (10) and (11) delineate the thresholds for the operation of active and reactive power flow within the microgrid, respectively.

$$- \overline{F}_{nm,t}^p \le F_{nm,t}^p \le \overline{F}_{nm,t}^p \forall t \in T, nm \in B \tag{10}$$
$$- \overline{F}_{nm,t}^q \le F_{nm,t}^q \le \overline{F}_{nm,t}^q \forall t \in T, nm \in B \tag{11}$$

Equations (12) and (13) define the voltage limits for the microgrid and reference bus, respectively. It's worth noting that the voltage is squared in this paper.

$$\underline{V}_n \le V_{n,t} \le \overline{V}_n \forall n \in N, t \in T \tag{12}$$
$$V_{n,t} = 1 \forall n = ref \tag{13}$$

Equation (14) illustrates the constraint on the operation of real power from DGs.

$$\underline{P}_n^{DG} \le P_{n,t}^{DG} \le \overline{P}_n^{DG} \forall n \in N, t \in T \tag{14}$$

Equations (15) to (19) encompass the modeling of energy storage systems within the microgrid. Equation (15) establishes the discharge power limit, while equation (16) delineates the charge power limit. Equation (17) represents the energy level in the battery, with equation (18) specifying the initial battery energy. Lastly, equation (19) outlines the limit on battery energy.

$$0 \le P_{n,t}^{ess,dis} \le C_n^{ess} \left(1 - z_{n,t} \right) \forall n \in N, t \in T,$$
$$z \in \{0, 1\} \tag{15}$$
$$0 \le P_{n,t}^{ess,ch} \le C_n^{ess} \left(z_{n,t} \right) \forall n \in N, t \in T, z \in \{0, 1\} \tag{16}$$
$$E_{n,t+1}^{ess} = E_{n,t}^{ess} + P_{n,t}^{ess,ch} \eta^{ess,ch} - P_{n,t}^{ess,dis} \eta^{ess,dis}$$
$$\forall n \in N, t \in T, z \in \{0, 1\} \tag{17}$$
$$E_{n,t}^{ess} = 0 \forall n \in N, t = 1 \tag{18}$$
$$\underline{soc}_n^{ess} C_n^{ess} \le E_{n,t}^{ess} \le s\bar{o}c_n^{ess} C_n^{ess} \forall n \in N, t \in T \tag{19}$$

Equation (20) defines the square of voltage in the microgrid, represented in a convex modeling framework.

$$V_{n,t} = V_{m,t} - 2 \left(R_{nm} f_{nm,t}^p + X_{nm} f_{nm,t}^q \right) \ \forall nm \in B, t \in T, n \in N \tag{20}$$

Equation (21) sets the operational limit for renewable energy resources in the microgrid, encompassing sources such as wind and PV resources.

$$0 \le P_{n,t}^{RE} \le \overline{P}_{n,t}^{RE} \forall n \in N, t \in T \tag{21}$$

Constraints (22) and (23) delineate the operational limits of the capacitor and shunt reactor within the microgrid, respectively.

$$0 \le Q_{n,t}^{sc} \le \overline{Q}_n^{sc} \varphi_{n,t} \forall n \in N, t \in T, \varphi \in \{0, 1\} \tag{22}$$
$$0 \le Q_{n,t}^{ShR} \le \overline{Q}_n^{ShR} \left(1 - \varphi_{n,t} \right) \forall n \in N, t \in T, \varphi \in \{0, 1\} \tag{23}$$

Equations (24) to (26) illustrate the determination of the OLTC tap setting and step for tap changes.

$$V_{n,t} = 1 \times \nabla_{n,t,m}^{oltc} \forall n \in \Omega^{OLTC}, t \in T, m \in M \tag{24}$$

$$\nabla_{n,t,m}^{oltc} = \sum_{m \in M} A_m \times \theta_{m,t}^{oltc} \forall n \in \Omega^{OLTC},$$
$$t \in T, m \in M, \theta \in \{0, 1\} \tag{25}$$

$$\sum_m \theta_{m,t}^{oltc} \le 1 \forall t \in T \tag{26}$$

Likewise, relationships (27) to (29) are applied for the SVR. It is noteworthy that the OLTC tap influences the reference bus of the microgrid, while the SVR tap impacts the voltage between two nodes.

$$V_{n,t} = V_{m,t} \times \nabla_{n,t,m}^{SVR} - 2 \left(R_{nm} F_{nm,t}^p + X_{nm} F_{nm,t}^q \right)$$
$$\forall n, m \in \Omega^{SVR}, t \in T, nm \in B \tag{27}$$

$$\nabla_{n,t,m}^{SVR} = \sum_{m \in M} B_m \times \theta_{m,t}^{SVR} \forall n \in \Omega^{SVR},$$
$$t \in T, m \in M, \theta \in \{0, 1\} \tag{28}$$

$$\sum_m \theta_{m,t}^{SVR} \le 1 \forall t \in T \tag{29}$$

Equations (30) and (31) depict the curtailment of active and reactive loads within the microgrid, respectively.

$$0 \le D_{n,t}^{p,shed} \le D_{n,t}^{p,DSM} \forall n \in N, t \in T \tag{30}$$
$$0 \le D_{n,t}^{q,shed} \le D_{n,t}^{q,DSM} \forall n \in N, t \in T \tag{31}$$

The upper and lower ramp rate limits for DGs are presented in equations (32) and (33), respectively.

$$P_{n,t+1}^{DG} - P_{n,t}^{DG} \le r^{up} \forall n \in N, t \in T \tag{32}$$
$$P_{n,t}^{DG} - P_{n,t+1}^{DG} \le r^{dw} \forall n \in N, t \in T \tag{33}$$

Finally, equations (34) to (37) delineate the optimal modeling for the charging and discharging of electric vehicles.

$$0 \le P_{n,t}^{EV,ch} \le \overline{P}_n^{EV,ch} \gamma_{n,t} \forall n \in N, t \in T \tag{34}$$
$$0 \le P_{n,t}^{EV,dis} \le \overline{P}_n^{EV,dis} \left(1 - \gamma_{n,t} \right) \forall n \in N, t \in T \tag{35}$$

$$E_{n,t+1}^{EV} = E_{n,t}^{EV} + P_{n,t+1}^{EV,ch} \eta_{EV}^{ch} - \frac{P_{n,t}^{EV,dis}}{\eta_{EV}^{dis}} \forall n \in N, t \in T \tag{36}$$

$$\overline{E}_n^{EV} \times E^{soc} \le E_{n,t}^{EV} \le \overline{E}_n^{EV} \forall n \in N, t \in T \tag{37}$$

III. PROPOSED ROBUST APPROACH

In practical scenarios, the operational scheduling problem of MG is typically addressed one day prior to the actual operation, which introduces various uncertainties into the planning process. These uncertainties can arise from unpredictable factors such as fluctuating renewable energy generation, varying load demands, equipment failures, and market price fluctuations. The unpredictable nature of renewable energy sources, such as solar and wind power, can lead to significant variability in energy generation, making it challenging to accurately forecast and plan energy dispatch schedules. Additionally, variations in consumer behavior, seasonal changes, and unexpected events can result in fluctuations in load demand,

requiring dynamic adjustments to the microgrid operation schedule. Unforeseen equipment failures or outages can impact the availability and reliability of DG, necessitating contingency plans and adaptive strategies. Moreover, fluctuations in electricity market prices can influence the economic dispatch decisions, requiring optimization models to consider cost-effective strategies while ensuring reliable operation. In conclusion, the proposed two-stage robust optimization model offers a comprehensive and adaptive approach to address uncertainties in microgrid operational scheduling effectively. By considering the range and variability of uncertainties in both day-ahead planning and real-time adaptation, the model ensures robust, reliable, and efficient microgrid operation under diverse operating conditions and uncertainties.

A. UNCERTAINTY MODELING
In the context of robust optimization, uncertainties are delineated through suitable uncertainty sets. For the microgrid load, this set (U_D^p, U_D^q) can be defined as follows:

$$U_D^p = \begin{cases} \tilde{D}_{n,t}^{p,INI} \in R^+ \left| \underline{\Gamma_t^{p,D}} \le \dfrac{\sum_n \tilde{D}_{n,t}^{p,INI}}{\sum_n D_{n,t}^{p,INI}} \le \overline{\Gamma}_t^{p,D}, \right. \\ \tilde{D}_{n,t}^{p,INI} \in \left[D_{n,t}^{p,INI} - D_{n,t}^{p,INI} \times \gamma, D_{n,t}^{p,INI} + D_{n,t}^{p,INI} \times \gamma \right] \end{cases} \tag{38}$$

$$U_D^q = \begin{cases} \tilde{D}_{n,t}^{q,INI} \in R^+ \left| \underline{\Gamma_t^{q,D}} \le \dfrac{\sum_n \tilde{D}_{n,t}^{q,INI}}{\sum_n D_{n,t}^{q,INI}} \le \overline{\Gamma}_t^{q,D}, \right. \\ \tilde{D}_{n,t}^{q,INI} \in \left[D_{n,t}^{q,INI} - D_{n,t}^{q,INI} \times \gamma, D_{n,t}^{q,INI} + D_{n,t}^{q,INI} \times \gamma \right] \end{cases} \tag{39}$$

According to equations (38, 39), the uncertain load varies within the interval $\left[D_{n,t}^{p,INI} - D_{n,t}^{p,INI} \times \gamma, D_{n,t}^{p,INI} + D_{n,t}^{p,INI} \times \gamma \right]$. To modify the conservation level of the optimal solution, the values of $\Gamma_t^{p,D}$ and $\Gamma_t^{q,D}$ (referred to as the uncertainty budget) can be adjusted. Specifically, as $\Gamma_t^{p,D}$ and $\Gamma_t^{q,D}$ increase from 0 to 24, the conservation level of the optimal solution increases. Consequently, the time during which the load at bus n can assume either its lower or upper bounds also increases. A similar uncertainty set can be defined for renewable power generation (U_G):

$$U_{RE} = \begin{cases} \tilde{P}_{n,t}^{RE} \in R^+ \left| \underline{\Gamma_t^{re}} \le \dfrac{\sum_n \tilde{D}_{n,t}^{p,INI}}{\sum_n P_{n,t}^{RE}} \le \overline{\Gamma}_t^{re}, \right. \\ \tilde{P}_{n,t}^{RE} \in \left[P_{n,t}^{RE} - \hat{P}_{n,t}^{RE}, P_{n,t}^{RE} + \hat{P}_{n,t}^{RE} \right] \end{cases} \tag{40}$$

where Γ_t^{re} represents the uncertainty budget for renewable power generation.

B. PROPOSED TWO-STAGE ROBUST MODEL
Taking into account the specified uncertainty sets, the formulation of the two-stage robust optimization-based model is as

follows:

$$\min_{x_t} \sum_{t \in T} a_t^T x_t + \max_{v_D^p, V_D^q, U_{RE}} \min_{y_t \in O(x_1, \ldots, x_T, i, d, g)} \sum_{t \in T} b_t^T y_t \quad (41)$$

$$C_t x_t \leq c_t \quad (42)$$

$$O(x_1, \ldots, x_T, i, d, g)$$
$$= \left\{ y_t \mid \begin{array}{l} H_t y_t \leq h_t \\ G_t y_t \leq L_t d_t - i_t x_t - E_t x_t - K_t g_t \\ N_t y_t \leq w - M_t x_t \end{array} \right\} \quad (43)$$

Here, x and y represent decision variables for operation modes. C, E, G, H, K, L, M, and N are auxiliary coefficients, while a, b, c, h, and w serve as auxiliary parameters in the concise robust model. i, d, and g denote the uncertainty realization of load demand and renewable generation, respectively. In the proposed two-stage robust model, the first-stage problem involves determining the robust energy scheduling of DGs, the energy scheduling of ESS, the energy scheduling of EV, the power scheduling of capacitors and reactors, and the tap scheduling of SVR and OLTC. This stage aims to minimize the total cost of the MG considering worst-case realizations. Once the first-stage decisions are established, the worst-case realization of the MG under uncertainties is computed through an inner *max-min* model, essentially addressing a resiliency-oriented problem.

Equation (42) delineates the feasible set for operation decision variables, encapsulating constraints (2)-(37). The initial inequality in (43) consolidates constraints exclusively related to operation decision variables, namely (4), (5), and (14). The subsequent inequality in (43) is strategically chosen to articulate constraints (2) and (3). Lastly, the concluding inequality in (43) defines the condensed representation of (32) and (33).

C. C&CG ALGORITHM FOR SOLVING TWO-STAGE RO MODEL

The *min–max–min* optimization problem presented in equations (41)-(43) poses a challenge for commercial software packages, rendering them insufficient for its resolution. Consequently, a C&CG algorithm, extensively detailed in [21], is employed to effectively address the proposed robust model. In contrast to alternative algorithms such as the BD algorithm [22], the C&CG algorithm demonstrates superior capabilities in solving master problems with a greater number of variables and constraints in fewer iterations [23]. Notably, the BD algorithm necessitates the subproblem to be in linear format, a prerequisite not applicable to the C&CG algorithm [21].

1) MASTER PROBLEM (MP)

$$\min_{x_t, \varphi} \varphi \quad (44)$$

$$C_t x_t \leq c_t \quad (45)$$

$$\varphi \geq \sum_{t \in T} a_t^T x_t + \sum_{t \in T} b_t^T y_t^\vartheta \quad (46)$$

$$H_t y_t^\vartheta \leq h_t \quad (47)$$

$$G_t y_t^\vartheta \leq L_t d_t^\vartheta - i_t^\vartheta x_t - E_t x_t - K_t g_t^\vartheta \quad (48)$$

$$N_t y_t^\vartheta \leq w - M_t x_t \quad (49)$$

Here, φ serves as an auxiliary variable, and ϑ represents the iteration index. The primary objective of the master problem is to identify the optimal first-stage decision based on the worst-case realizations determined in the sub-problem. Consequently, the master problem establishes a lower bound for the two-stage robust optimization-based model presented in equations (41)-(43).

2) SUB-PROBLEM (SP)

The sub-problem is designed to ascertain the worst-case realization within the specified uncertainty sets. Specifically, for the first-stage optimal robust decisions, denoted as x_t^*, the sub-problem is formulated as follows:

$$\eta(x^*) = \max_{d \in U_D^p, i \in U_D^q, g \in U_{RE}} \min_{y_t \in L(x_1, \ldots, x_T, i, d, g)} \sum_{t \in T} b_t^T y_t \quad (50)$$

$$H_t y_t \leq h_t (\pi_t) \quad (51)$$

$$G_t y_t \leq L_t d_t - i_t x_t^* - E_t x_t^* - K_t g_t (\gamma_t) \quad (52)$$

$$N_t y_t \leq w - M_t x_t^* (\omega_t) \quad (53)$$

Here, η stands as an auxiliary variable, while π, γ, and ω serve as dual variables for constraints (51)-(53), respectively. The aforementioned *max-min* problem establishes an upper bound for the two-stage robust optimization-based model outlined in equations (41)-(43). However, direct optimization of this problem is not feasible. Fortunately, due to the linearity of the sub-problem, the application of duality theory allows it to be expressed as follows:

$$\max_{\pi, \gamma, \omega, i, d, g} \sum_{t \in T} \left\{ h_t^T \pi_t + \left(L_t d_t - I_t x_t^* - E_t x_t^* - K_t g_t \right)^T \gamma_t \right.$$
$$\left. + \left(w + M_t x_t^* \right)^T \omega_t \right\} \quad (54)$$

$$H_t^T \pi_t + G_t^T \gamma_t + N_t^T \omega_t = b_t \quad (55)$$

$$\pi_t \leq 0, \gamma_t \leq 0, \omega_t \leq 0 \quad (56)$$

$$d_t \in U_D^p, i_t \in U_D^q, g_t \in U_{RE} \quad (57)$$

After solving the derived equivalent formulation for the sub-problem, the worst-case realization is determined over the uncertainty sets in each iteration, and the associated constraints (46)-(49) are integrated into the master problem. The iterative process terminates when the difference between the upper and lower bounds diminishes to a predefined threshold. Refer to Fig. 1 for the flowchart illustrating the proposed solution algorithm. In fact, the two-stage model arises because the optimization problem is divided into a master problem and a sub-problem, as depicted in the proposed flowchart in Figure 1. The main purpose of presenting this model is to operate microgrids while taking into account the considered uncertainties.

IV. NUMERICAL RESULTS

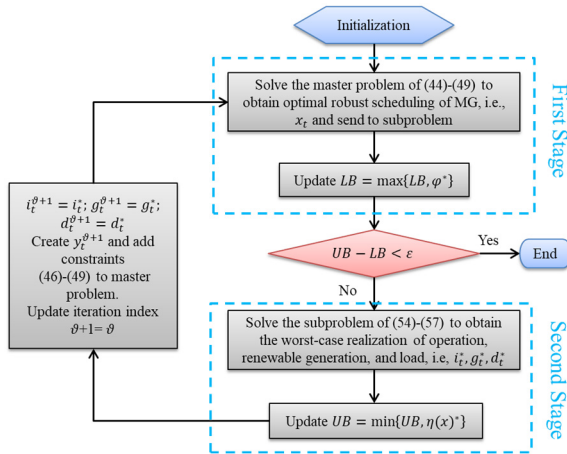The proposed approach and model were implemented to evaluate the performance of a 33-bus microgrid infrastructure

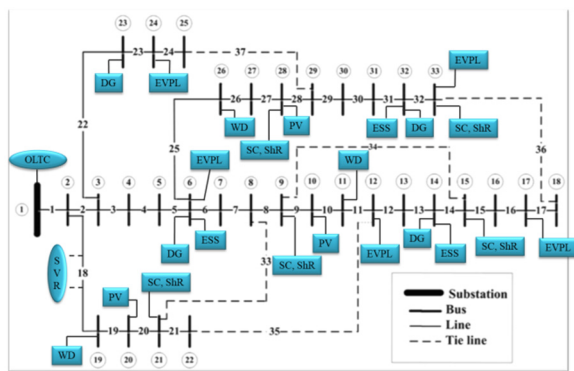**FIGURE 1.** Flowchart of the proposed two-stage solution algorithm.

FIGURE 2. Proposed microgrid schematic.

TABLE 3. Island mode result.

	Proposed	Method 1 in [24]	Method 2 in [25]
Objective ($)	90154	97005	94660
Energy purchase (MWh)	0	0	0
Loss (MWh)	0.312	0.339	0.324
Load shedding (MWh)	0.978	1.68	1.03
Voltage deviation (p.u)	0.057	0.061	0.059
PV curtailment (MWh)	0.78	1.21	1.04
WD curtailment (MWh)	0	0	0
Peak of charge of ESS (MWh)	0.45	0.51	0.47
Total power of the SC (MVArh)	12.43	12.79	12.62
Total power of the ShR (MVArh)	10.57	10.84	10.74
CPU time (sec)	154	116	81

Regarding energy metrics, the proposed method achieves an energy purchase of 0.45 MWh, which is lower than that of Method 1 (0.474 MWh) and Method 2 (0.468 MWh). Additionally, the proposed method effectively minimizes losses (0.387 MWh), load shedding (0.16 MWh), and voltage deviation (0.065 p.u) compared to the other methods. The proposed method demonstrates superior performance in managing renewable resources, with lower PV curtailment (2.25 MWh) and no wind curtailment (0 MWh), whereas Method 1 and Method 2 experience higher curtailment values. For energy ESS operations, the proposed method achieves a lower peak charge (0.56 MWh) compared to Method 1 (0.59 MWh) and Method 2 (0.58 MWh). Furthermore, the proposed method optimizes the total power of the SC and ShR more efficiently, resulting in 10.66 MVArh and 11.4 MVArh, respectively. Lastly, the computational efficiency of the proposed method is evident in the CPU time required, which is 131 seconds, compared to 97 seconds for Method 1 and 61 seconds for Method 2. Overall, these results collectively demonstrate the effectiveness and efficiency of the proposed method in optimizing the grid-connected mode of the microgrid.

Table (3) presents the results of the islanded mode using the proposed method, compared with Method 1 from [24] and Method 2 from [25]. The objective function, representing the total cost, is minimized by the proposed method, resulting in a cost of $90,154. In contrast, Method 1 and Method 2 produce higher costs of $97,005 and $94,660, respectively. Regarding energy metrics, the proposed method achieves zero energy purchase, losses of 0.312 MWh, and load shedding of 0.978 MWh, demonstrating its effectiveness in ensuring energy self-sufficiency during islanded mode operation. In comparison, Method 1 and Method 2 show nonzero values for these metrics, indicating less efficient resource utilization in islanded mode. The proposed method excels in minimizing voltage deviation (0.057 p.u) during islanded mode, outperforming Method 1 (0.061 p.u) and Method 2 (0.059 p.u). In managing renewable resources during islanded

[31]. Figure 2 presents a schematic representation of the microgrid, highlighting key components such as electric vehicle parking, energy storage systems, distributed generation sources, and renewable energy sources. Notably, the model considers active and reactive demand modifications with a maximum allowable deviation of 20%. For this study, energy storage systems and electric vehicle batteries are assumed to be lithium-based, with an operational efficiency of 95%. To conduct the simulation, we employed the proposed method and model implemented in Julia and solved it using Gurobi 10. The 33-node microgrid illustrated in Figure 2 consists of 32 lines, underscoring the presence of various elements, including PV resources, WD, EVPL, ESS, SC, ShR, OLTC, SVR, and DG resources.

Table (2) displays the results of the grid-connected mode using the proposed method, compared to Method 1 (based on the Genetic algorithm) from [24] and Method 2 (based on the Particle Swarm Optimization algorithm) from [25]. The objective function, which represents the total cost, is minimized by the proposed method, resulting in a cost of $86,978. In contrast, Method 1 and Method 2 yield higher costs of $93,936 and $91,326, respectively.

mode, the proposed method achieves lower PV curtailment (0.78 MWh) compared to Method 1 (1.21 MWh) and Method 2 (1.04 MWh). Wind curtailment remains zero across all methods, indicating efficient utilization of wind resources. For energy storage system (ESS) operations, the proposed method optimizes the peak charge, resulting in a lower value of 0.45 MWh compared to Method 1 (0.51 MWh) and Method 2 (0.47 MWh). Additionally, the proposed method optimizes the total power of the shunt capacitor (SC) and shunt reactor (ShR) more effectively, resulting in values of 12.43 MVArh and 10.57 MVArh, respectively. The computational efficiency of the proposed method is reflected in the CPU time required, which is 154 seconds, compared to 116 seconds for Method 1 and 81 seconds for Method 2. Overall, these results highlight the effectiveness and efficiency of the proposed method in optimizing the islanded mode of the microgrid, emphasizing its capability to ensure self-sufficiency and reliability during periods of disconnection from the main grid.

The comprehensive evaluation of the grid-connected and islanded modes, presented in Tables (2) and (3), offers valuable insights into the performance of the proposed microgrid optimization method compared to existing methodologies (Method 1 from [24] and Method 2 from [25]). In the grid-connected mode, the proposed method demonstrates superior economic efficiency by minimizing the objective function to $86,978, surpassing the results of Method 1 ($93,936) and Method 2 ($91,326). This cost-effectiveness stems from optimized energy purchases, reduced losses, and minimized load shedding, highlighting the method's adept management of energy resources. Additionally, the proposed method excels in mitigating voltage deviations, curtailing PV generation, and efficiently operating the ESS, resulting in lower peak charges. The optimized total power of the SC and ShR enhances overall system performance. Importantly, the proposed method achieves these outcomes within a reasonable computational time of 131 seconds, emphasizing its efficiency for real-time applications. In the islanded mode, the proposed method continues to demonstrate its effectiveness by minimizing the objective function to $90,154, outperforming Method 1 ($97,005) and Method 2 ($94,660). The method's capability to completely eliminate energy purchases while maintaining minimal losses and load shedding highlights its effectiveness in ensuring energy self-sufficiency during islanded operation. Moreover, the proposed method excels in voltage regulation, reducing PV curtailment, and optimal ESS management, contributing to enhanced resilience of the islanded microgrid. The optimized total power of SC and ShR further emphasizes the method's ability to maximize renewable resource utilization. The computational efficiency of the proposed method remains reasonable at 154 seconds, ensuring its practical applicability in real-world scenarios. In summary, the proposed microgrid optimization method not only surpasses existing methodologies in economic efficiency, renewable resource utilization, and voltage regulation but also maintains
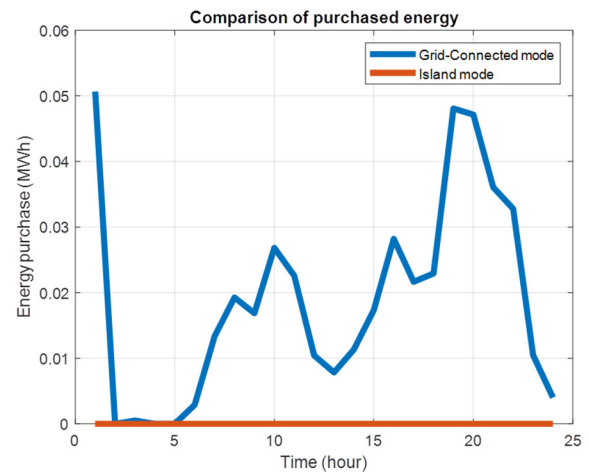
FIGURE 3. Comparison of purchased energy between grid-connected and island modes.

commendable computational efficiency. Collectively, these results affirm the method's viability and effectiveness in addressing the complex challenges associated with microgrid operation in both grid-connected and islanded modes.

Figure (3) presents a comparative line graph showing the average energy consumption in grid-connected and islanded modes over time. In this visual representation, the grid-connected mode appears as the more expensive option, whereas the islanded mode emerges as the more economical choice. The x-axis of the graph represents time in hours, while the y-axis indicates energy purchases measured in MWh. The two distinct lines on the graph represent the average energy consumption trends for the grid-connected and islanded modes, respectively. As shown in the graph, the grid-connected mode demonstrates higher energy consumption compared to the islanded mode. This difference stems from the continuous need to purchase energy from the grid in the grid-connected mode, even during periods of reduced demand. In contrast, the islanded mode relies solely on locally generated energy, eliminating the need for external energy procurement. This comparison underscores the significant energy-saving potential of the islanded mode, positioning it as a more cost-effective and sustainable option for energy consumption.

Figure (4) depicts a graph comparing the average microgrid voltage between grid-connected and islanded modes. The x-axis of the graph represents time in hours, while the y-axis indicates voltage magnitude in per unit (p.u.). The graph illustrates that the grid-connected mode maintains a higher average voltage compared to the islanded mode. This difference arises because the grid-connected mode is linked to the main power grid, which provides a stable voltage. In contrast, the islanded mode operates independently of the main power grid, leading to voltage fluctuations based on the microgrid's power generation and consumption levels. The graph also reveals that the voltage magnitude in both the grid-connected and islanded modes fluctuates over time. Various
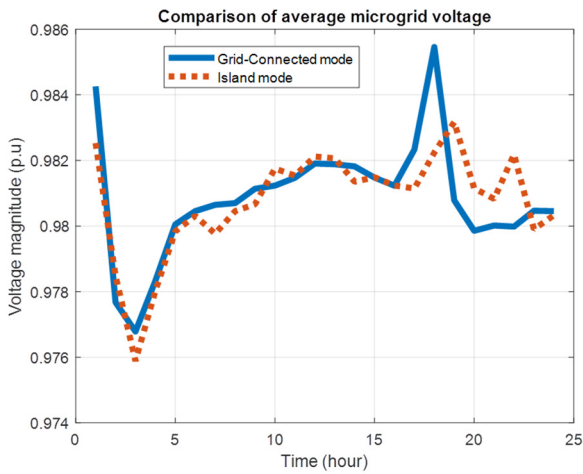
FIGURE 4. Comparison of average microgrid voltage between grid-connected and island modes.
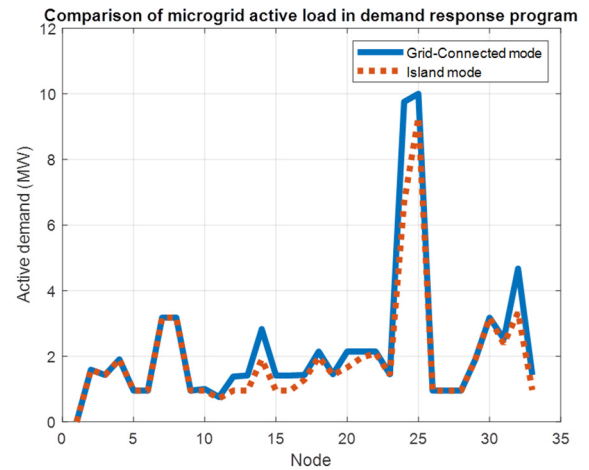

FIGURE 6. Comparison of microgrid active load in demand response programs.
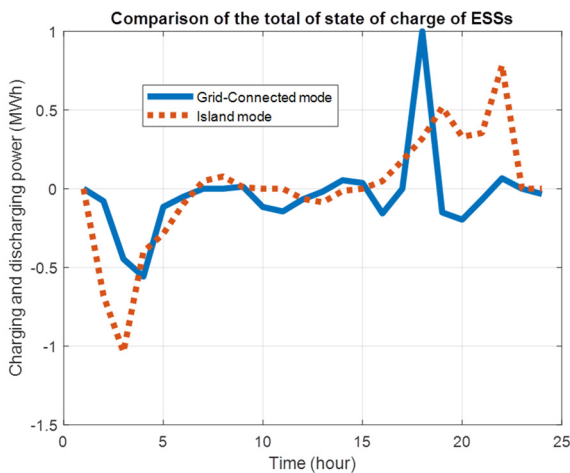

**FIGURE 5.** Comparison of the total of state of charge of grid-connected and island-mode ESSs over time.

factors, such as the load on the microgrid, can influence the voltage of both modes. Overall, the figure demonstrates that the grid-connected mode maintains a higher and more consistent voltage compared to the islanded mode.

Figure (5) presents a line graph comparing the total state of charge of grid-connected and islanded ESSs over time. The x-axis of the graph represents time in hours, while the y-axis indicates the state of charge as a percentage. The graph illustrates that the islanded ESSs maintain a higher total state of charge compared to the grid-connected ESSs. This difference arises because the islanded ESSs are responsible for supplying all the energy to the microgrid, whereas the grid-connected ESSs can draw energy from the grid when required. The graph also reveals that the total state of charge for both grid-connected and islanded ESSs fluctuates over time. This fluctuation occurs because the state of charge for both types of ESSs depends on the amount of energy generated and consumed by the microgrid. Overall, the figure

demonstrates that the islanded ESSs maintain a higher total state of charge than the grid-connected ESSs, indicating that the islanded ESSs can store more energy. This stored energy can be utilized to power the microgrid during periods of low or no renewable energy generation.

Figure (6) presents a visual comparison of load profiles within the demand-side management program in two distinct modes: islanded and grid-connected. Remarkably, the islanded mode shows instances of load shedding, particularly at nodes 12-16, 24, 25, 33, and 32. This observation highlights a significant difference in load reduction between the islanded and grid-connected modes. The noticeable pattern of load shedding in the islanded mode indicates a more pronounced and effective reduction in overall load demand compared to the grid-connected mode. This result aligns with the inherent advantages of islanded operation, where the microgrid autonomously manages and optimizes its load distribution, showcasing its resilience and ability to adapt to varying demand scenarios. The visual representation in Figure (6) offers valuable insights into the contrasting load dynamics, confirming the efficiency and flexibility provided by the islanded mode in demand-side management.

Figure (7) displays a comprehensive line graph illustrating the hourly energy trends of EVs in both grid-connected and islanded modes over time. The x-axis of the graph represents time in hours, while the y-axis measures energy in MWh. The graph clearly shows that the energy consumption of grid-connected EVs exceeds that of islanded-mode EVs. A closer look at the graph reveals dynamic fluctuations in the energy consumption of both grid-connected and islanded-mode EVs throughout the observed period. These variations can be attributed to several influencing factors, such as the time of day, the day of the week, and prevailing weather conditions. The complex interaction of these elements highlights the intricate nature of energy consumption patterns for both types of EVs. The visual representation in Figure (7) serves as a
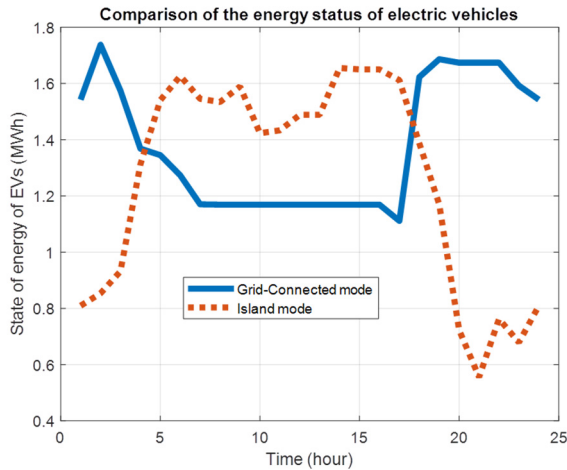
FIGURE 7. Comparison of the hourly state of energy of EVs of grid-connected and island-mode.

valuable tool for understanding the nuanced dynamics of EV energy consumption, providing insights into the impact of operational conditions on their energy usage.

V. CONCLUSION

Managing energy in microgrids is a complex and challenging endeavor due to the uncertainties linked to renewable energy resources, fluctuating demand, and a variety of devices. This paper introduces a sophisticated two-stage robust day-ahead optimization model designed specifically for microgrid operations. The model tackles challenges associated with integrating power electronic-based generation units, managing uncertain demand within microgrids, and incorporating small-scale renewable energy resources. It includes detailed formulations for microgrid energy management, covering optimal battery usage, efficient EV energy management, compensator usage, and strategic dispatching of DG resources. The multi-objective function aims to minimize various costs, including energy losses, power purchases, load curtailment, DG operation, and expenses related to batteries and EVs over a 24-hour period.

The optimization problem is efficiently solved using a C&CG algorithm. Numerical simulations carried out on a test system confirm the effectiveness of the proposed model and solution algorithm, showing a notable reduction in the operating costs of the microgrid. The proposed approach offers a robust framework to strengthen the resilience and improve the efficiency of microgrid energy management. The results clearly demonstrate that the proposed approach surpasses comparable methods by at least 5%, highlighting its effectiveness in enhancing key performance indicators within the microgrid system.

Overall, the proposed approach represents a significant advancement in microgrid energy management, providing a robust and efficient framework to reduce operating costs, strengthen resilience, and improve efficiency.

It addresses the key challenges of microgrid energy management, including the integration of power electronic-based generation units, the uncertain nature of demand, and the incorporation of small-scale renewable energy resources.

∗ It features meticulous formulations for optimal battery utilization, efficient EV energy management, compensator utilization, and strategic dispatching of DG resources.

∗ It employs a C&CG algorithm to efficiently solve the complex optimization problem.

∗ It demonstrates significant cost savings and improved performance over comparable methods.

The proposed approach presents a promising foundation for future research in microgrid energy management. Potential areas for further exploration include:

∗ Developing more sophisticated uncertainty modeling techniques to account for a wider range of factors, such as weather conditions and market prices.

∗ Investigating the use of machine learning and artificial intelligence to improve the efficiency and accuracy of the optimization process.

∗ Exploring the integration of the proposed approach with other microgrid management systems, such as demand response and fault tolerance mechanisms.

Overall, the proposed approach represents a significant step forward in microgrid energy management, offering a robust and efficient framework to minimize operating costs, fortify resilience, and enhance efficiency. It provides a solid foundation for future research in this important and rapidly developing field.

REFERENCES

[1] V. Gali, P. K. Jamwal, N. Gupta, and A. Kumar, "An adaptive dynamic power management approach for enhancing operation of microgrid with grid ancillary services," *Renew. Energy*, vol. 219, Dec. 2023, Art. no. 119413.

[2] F. N. Budiman, M. A. M. Ramli, H. R. E. H. Bouchekara, and A. H. Milyani, "Optimal scheduling of a microgrid with power quality constraints based on demand side management under grid-connected and islanding operations," *Int. J. Electr. Power Energy Syst.*, vol. 155, Jan. 2024, Art. no. 109650.

[3] V. Shahbazbegian, M. Shafie-khah, H. Laaksonen, G. Strbac, and H. Ameli, "Resilience-oriented operation of microgrids in the presence of power-to-hydrogen systems," *Appl. Energy*, vol. 348, Oct. 2023, Art. no. 121429.

[4] X. Chen, J. Zhai, Y. Jiang, C. Ni, S. Wang, and P. Nimmegeers, "Decentralized coordination between active distribution network and multi-microgrids through a fast decentralized adjustable robust operation framework," *Sustain. Energy, Grids Netw.*, vol. 34, Jun. 2023, Art. no. 101068.

[5] Ö. Erol and Ü. Başaran Filik, "A Stackelberg game-based dynamic pricing and robust optimization strategy for microgrid operations," *Int. J. Electr. Power Energy Syst.*, vol. 155, Jan. 2024, Art. no. 109574.

[6] B. Cortés-Caicedo, L. F. Grisales-Noreña, O. D. Montoya, and R. I. Bolaños, "Optimization of BESS placement, technology selection, and operation in microgrids for minimizing energy losses and CO_2 emissions: A hybrid approach," *J. Energy Storage*, vol. 73, Dec. 2023, Art. no. 108975.

[7] Z. Li, B. Zhao, Z. Chen, C. Ni, J. Yan, X. Yan, X. Bian, and N. Liu, "Low-carbon operation method of microgrid considering carbon emission quota trading," *Energy Rep.*, vol. 9, pp. 379–387, Apr. 2023.

[8] M. H. Parvaneh, M. H. Moradi, and S. M. Azimi, "The advantages of capacitor bank placement and demand response program execution on the optimal operation of isolated microgrids," *Electr. Power Syst. Res.*, vol. 220, Jul. 2023, Art. no. 109345.

[9] Y. Li, X. Zhang, Y. Wang, X. Qiao, S. Jiao, Y. Cao, Y. Xu, M. Shahidehpour, and Z. Shan, "Carbon-oriented optimal operation strategy based on Stackelberg game for multiple integrated energy microgrids," *Electr. Power Syst. Res.*, vol. 224, Nov. 2023, Art. no. 109778.

[10] Z. Guo, W. Wei, J. Bai, and S. Mei, "Long-term operation of isolated microgrids with renewables and hybrid seasonal-battery storage," *Appl. Energy*, vol. 349, Nov. 2023, Art. no. 121628.

[11] J. Xu and Y. Yi, "Multi-microgrid low-carbon economy operation strategy considering both source and load uncertainty: A Nash bargaining approach," *Energy*, vol. 263, Jan. 2023, Art. no. 125712.

[12] Z. Shi, T. Zhang, Y. Liu, Y. Feng, R. Wang, and S. Huang, "Optimal design and operation of islanded multi-microgrid system with distributionally robust optimization," *Electr. Power Syst. Res.*, vol. 221, Aug. 2023, Art. no. 109437.

[13] D. Krupenev, N. Komendantova, D. Boyarkin, and D. Iakubovskii, "Digital platform of reliability management systems for operation of microgrids," *Energy Rep.*, vol. 10, pp. 2486–2495, Nov. 2023.

[14] Z. Liang, Z. Dong, C. Li, C. Wu, and H. Chen, "A data-driven convex model for hybrid microgrid operation with bidirectional converters," *IEEE Trans. Smart Grid*, vol. 14, no. 2, pp. 1313–1316, Mar. 2023.

[15] O. M. Adeyanju, P. Siano, and L. N. Canha, "Dedicated microgrid planning and operation approach for distribution network support with pumped-hydro storage," *IEEE Trans. Ind. Informat.*, vol. 19, no. 7, pp. 8229–8241, Jul. 2023.

[16] L. Tang, E. Shang, X. Chen, L. Li, and S. Zou, "Optimization effect analysis of ACM-PSO integrating individual adjustment and cross operation on microgrid DG technology," *IEEE Access*, vol. 11, pp. 59954–59967, 2023.

[17] Y. Wang, Y. Li, Y. Cao, M. Shahidehpour, L. Jiang, Y. Long, Y. Deng, and W. Li, "Optimal operation strategy for multi-energy microgrid participating in auxiliary service," *IEEE Trans. Smart Grid*, vol. 14, no. 5, pp. 3523–3534, Sep. 2023.

[18] D. A. Quijano, M. Vahid-Ghavidel, M. S. Javadi, A. Padilha-Feltrin, and J. P. S. Catalão, "A price-based strategy to coordinate electric springs for demand side management in microgrids," *IEEE Trans. Smart Grid*, vol. 14, no. 1, pp. 400–412, Jan. 2023.

[19] G. Abdulnasser, A. Ali, M. F. Shaaban, and E. E. M. Mohamed, "Optimizing the operation and coordination of multi-carrier energy systems in smart microgrids using a stochastic approach," *IEEE Access*, vol. 11, pp. 58470–58490, 2023.

[20] L. Ahmethodžić, M. Music, and S. Huseinbegovic, "Microgrid energy management: Classification, review and challenges," *CSEE J. Power Energy Syst.*, vol. 9, no. 4, pp. 1425–1438, Jul. 2023.

[21] B. Zeng and L. Zhao, "Solving two-stage robust optimization problems using a column-and-constraint generation method," *Oper. Res. Lett.*, vol. 41, no. 5, pp. 457–461, Sep. 2013.

[22] S. Dehghan, N. Amjady, and A. Kazemi, "Two-stage robust generation expansion planning: A mixed integer linear programming model," *IEEE Trans. Power Syst.*, vol. 29, no. 2, pp. 584–597, Mar. 2014.

[23] Y. Guo and C. Zhao, "Islanding-aware robust energy management for microgrids," *IEEE Trans. Smart Grid*, vol. 9, no. 2, pp. 1301–1309, Mar. 2018.

[24] Y. Qu, H. Wang, J. Wu, X. Yang, H. Yin, and L. Zhou, "Robust optimization of train timetable and energy efficiency in urban rail transit: A two-stage approach," *Comput. Ind. Eng.*, vol. 146, Aug. 2020, Art. no. 106594.

[25] H. J. Kim, M. K. Kim, and J. W. Lee, "A two-stage stochastic *p*-robust optimal energy trading management in microgrid operation considering uncertainty with hybrid demand response," *Int. J. Electr. Power Energy Syst.*, vol. 124, Jan. 2021, Art. no. 106422.

[26] P. Sharma, K. K. Saini, H. D. Mathur, and P. Mishra, "Improved energy management strategy for prosumer buildings with renewable energy sources and battery energy storage systems," *J. Mod. Power Syst. Clean Energy*, vol. 12, no. 2, pp. 381–392, 2024.

[27] Y. Akarne, A. Essadki, T. Nasser, and B. E. Bhiri, "Experimental analysis of efficient dual-layer energy management and power control in an AC microgrid system," *IEEE Access*, vol. 12, pp. 30577–30592, 2024.

[28] M. Abdelsattar, M. A. Ismeil, M. M. Aly, and S. S. Abu-Elwfa, "Energy management of microgrid with renewable energy sources: A case study in hurghada Egypt," *IEEE Access*, vol. 12, pp. 19500–19509, 2024.

[29] J. Hu, Y. Shan, Y. Yang, A. Parisio, Y. Li, N. Amjady, S. Islam, K. W. Cheng, J. M. Guerrero, and J. Rodríguez, "Economic model predictive control for microgrid optimization: A review," *IEEE Trans. Smart Grid*, vol. 15, no. 1, pp. 472–484, Jan. 2024.

[30] L.-N. Liu, G.-H. Yang, and S. Wasly, "Distributed predefined-time dual-mode energy management for a microgrid over event-triggered communication," *IEEE Trans. Ind. Informat.*, vol. 20, no. 3, pp. 3295–3305, Mar. 2024.

[31] S. H. Dolatabadi, M. Ghorbanian, P. Siano, and N. D. Hatziargyriou, "An enhanced IEEE 33 bus benchmark test system for distribution system studies," *IEEE Trans. Power Syst.*, vol. 36, no. 3, pp. 2565–2572, May 2021.

HAMID HEMATIAN received the master's degree from Islamic Azad University, Shahroord Branch, in 2014. He is currently pursuing the Ph.D. degree in electrical engineering with Islamic Azad University, Semnan Branch.

MOHAMAD TOLOU ASKARI received the Ph.D. degree in electrical engineering from Ferdowsi University. Since 2013, he has been a Faculty Member with Islamic Azad University, Shahrood Branch.

MEYSAM AMIR AHMADI received the Ph.D. degree in electrical engineering from Islamic Azad University Science and Research. Since 2014, he has been a Faculty Member with Islamic Azad University, Gorgan Branch.

MAHMOOD SAMEEMOQADAM received the master's degree from the University of Sistan and Blouchestan, in 2004, and the Ph.D. degree in electrical engineering from Tehran University of Technology, Tehran, Iran, in 2014. Since 2005, he has been a Faculty Member with Islamic Azad University, Shahrood Branch. He has published numerous articles in the field of electrical engineering.

MAJID BABAEI NIK received the Ph.D. degree in electrical engineering. Since 2010, he has been a Faculty Member with Islamic Azad University, Semnan Branch.

● ● ●